Pressure Dependence of Secondary Transitions in Amorphous Polymers. 4. T_{ll} from Isobaric V–T Data at $P \leq 600$ bars

Raymond F. Boyer

Michigan Molecular Institute, Midland, Michigan 48640. *Received October 7, 1980; Revised Manuscript Received May 16, 1982*

ABSTRACT: Available literature data on specific volume, V_{sp}, as a function of temperature at $P = 1$ bar were examined by regression analysis, with particular emphasis on residuals patterns. Such data do not follow second- or third-degree polynomials exactly but describe rather two straight lines intersecting at the liquid–liquid temperature, T_{ll}. In some cases, two intersecting quadratics provide a better fit. The change in coefficient of expansion, $\Delta\alpha$, across T_{ll} is calculated and compared with $\Delta\alpha$ across T_g as a measure of the strength of the T_{ll} transition compared to T_g. $\Delta\alpha$ at T_g is 2–25 times that at T_{ll}. T_{ll} is strongest in the poly(alkyl and cycloalkyl methacrylates), weakest in polystyrene and poly(vinyl acetate), and intermediate in atactic polypropylene. In addition, plots of V_{sp} or $1 - V/V_0$ against T at moderate pressures, 1 bar $< P \leq 600$ bars, reveal T_{ll} as slope changes. V is the specific volume at pressure P and V_0 is a reference volume at $P = 1$ or 0 bar. T_{ll} is presented graphically as a function of P for six polymers whose pressure coefficients, dT_{ll}/dP, are shown. This study provides thermodynamic-type evidence for T_{ll} similar to what has been available for T_g. It supplements T_{ll}–P results at higher pressures obtained previously from analysis of isothermal V–P data.

Introduction

Previous papers in this series were concerned with determination of a liquid–liquid transition, at temperature T_{ll}, as a function of pressure, using variations of and approximations to the Tait equation to analyze isothermal V–P data.[1,2] We noted that isobaric V–T data could be used, but only at low pressures, usually ≤400–500 bars, as suggested in Figure 1 of ref 1. We subsequently realized that the isothermal V–P method had limitations at low pressures because of insufficient data points below P = 400–500 bars to locate a transition pressure with accuracy. Thus the isobaric V–T method herein studied has the capability of supplementing the V–P approach. We have more recently shown that temperature variation of the Tait equation parameter, b, at $P \rightarrow 0$ can be used to locate T_{ll} at $P \rightarrow 0$.[3]

These several values of T_{ll} at low pressures are important in helping to define the locus of T_{ll}–P, which may be obscured in the region of P = 400–800 by interference from the T_g(LP) transition for some polymers. Inspection of Figure 2 in ref 1 indicates that such confusion may arise if dT_{ll}/dP is relatively small while $dT_g(\text{LP})/dP$ is relatively high.

We are now[4] employing a linear form of the Tait equation coupled with regression analysis to locate liquid-state transitions as a function of pressure more accurately than can be done by the methods employed in ref 1 and 2. The several common liquid-state transitions, as defined in Figure 2 of ref 1, include not only T_{ll} but a low-pressure glass transition, T_g(LP), the β relaxation and, more rarely, $T_{ll'}$ lying above T_{ll}.

Figure 1 is a plot of specific volume, V_{sp} (in cm^3 g^{-1}), as a function of temperature for poly(n-butyl methacrylate) at $P = 1$ bar, using the data of Olabisi and Simha.[5] We indicate three straight lines above T_g, with intersection at $T_{ll} \sim 95$ °C and $T_{ll'}$ at about 160–165 °C. A recent comprehensive review on these two transitions (relaxations),[6] as well as several earlier reviews,[7,9] provides background on the nature of both T_{ll} and $T_{ll'}$. Briefly, we consider T_{ll} to be of intermolecular origin and $T_{ll'}$ to be of intramolecular origin involving barriers to rotation about the polymer chain.[6,9]

Liquid-state V_{sp}–T data are characterized by Olabisi and Simha[5] for several polymers, including PnBMA, as third-degree polynomials. We shall demonstrate later that while the polynomial is a very good approximation to the data, it does not provide a true description of the actual numerical V_{sp}–T values.

This study is divided into two main sections: part I, isobaric V–T at $P = 1$; and part II, isobaric V–T data at $1 < P \leq 600$ bars. Our purpose in part I, aside from locating T_{ll}, is to determine slope changes, $\Delta\beta$, across T_{ll}, where $\Delta\beta = \beta_{ll} - \beta_l$, with β_{ll} being the slope above T_{ll}, namely, dV_{sp}/dT (in cm^3 g^{-1} K^{-1}), and β_l the corresponding quantity just below T_{ll} but above T_g. The β's are then converted to coefficients of expansion, α's (in K^{-1}), through division by V_{ll}, the specific volume at T_{ll}. $\Delta\alpha$ at T_{ll} is then compared with $\Delta\alpha$ at T_g to provide for the first time a numerical measure of the relative strengths of T_g and T_{ll} for each of eight polymers.

$\Delta\alpha$ at T_g has long been used as a measure of the strength of the glass-to-rubber transition in several different manners: (1) as a function of pressure, as shown by Gee for polystyrene[10] and by McKinney and Goldstein for poly(vinyl acetate);[11] (2) in the several Ehrenfest relationships, as discussed in most papers on P–V–T, for example, ref 10; (3) to compare the relative strengths of T_g and glassy-state transitions, as by Simha et al.[12–14]; and (4) in the several Simha–Boyer relationships

$$\Delta\alpha T_g = A + BT_g \tag{1}$$

where B may be zero[15–17] and A has a value near 0.11. Hence the precedent established with $\Delta\alpha$ at T_g suggested the validity of using $\Delta\alpha$ at T_{ll} as a measure of the absolute strength of the liquid–liquid transition. Hence the ratio ($\Delta\alpha$ at T_g)/($\Delta\alpha$ at T_{ll}) is calculated to indicate the strength of T_{ll} relative to T_g and is given in Table IV.

In part II, our main concern is in locating T_{ll} values for each of several isobars so as to obtain T_{ll}–P plots at low pressures for those polymers where data permit.

Methodology for $P = 1$

All sets of V_{sp}–T data at $T >$ – V_{sp}(calcd). P from 1 bar to about 600 bars are examined by computerized regression analysis, with particular emphasis on residuals patterns. A residual, symbol RES, is defined as V_{sp}(obsd) – V_{sp}(calcd). The latter is for a specific model selected to represent the data, i.e., linear, two line, three line, quadratic, etc. More generally, we use RES/SE, where SE is the standard error in V_{sp}(calcd). Plots of RES/SE against

0024-9297/82/2215-1498$01.25/0 © 1982 American Chemical Society

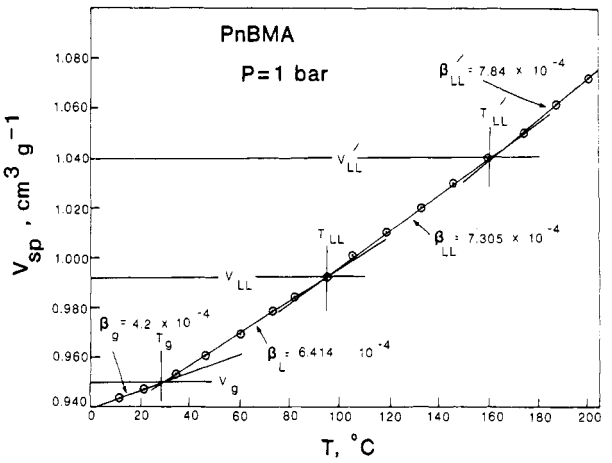

Figure 1. Specific volume–temperature plot for poly(*n*-butyl methacrylate) using the data of Olabisi and Simha at $P = 1$ bar.[5] Slope changes above T_g indicate T_{II} and $T_{II'}$. Slopes, β, and specific volumes at each transition are designated. Numerical values of the β's, all in units of cm^3 g^{-1} K^{-1}, are from this study. V_g, V_{II}, and $V_{II'}$ are specific volumes at the respective transition temperatures.

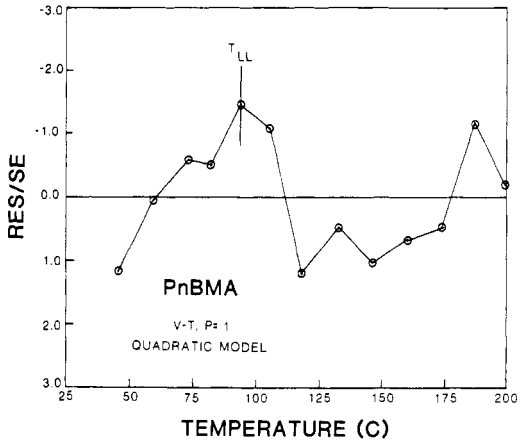

Figure 2. Nonrandom residuals/standard error (RES/SE) pattern for a quadratic model applied to the $T > T_g$ data of Figure 1. A nonrandom pattern is also found for a cubic model.

T should be random about zero and fall within ±2 if the correct model has been chosen. Incorrect models give nonrandom RES/SE–T plots. The specific procedures we employ have been described elsewhere[18] in considerable detail, and specific examples on various types of data have been shown.[6,8,9] In addition, modern textbooks on the use of residuals are available.[19,20] The usual symbolism is $(Y - \hat{Y})/\mathrm{SE}(\hat{Y})$, where $\hat{Y}$ signifies a calculated value of Y. We may also quote standard errors and coefficients of correlation but the final arbiter is the residuals pattern if sufficient data points exist.

To illustrate, Figure 2 shows the RES/SE pattern when a quadratic model is applied to the V_{sp}–T data for PnBMA plotted in Figure 1. The largest residuals occur first near 94.5–105.6 °C, i.e., in the vicinity of T_{II}, and then around 150–170 °C, i.e., near $T_{II'}$. The cubic model gives RES/SE values that are smaller than for the quadratic model but still nonrandom about zero. As we have noted on a prior occasion,[18] if the RES/SE pattern for a quadratic is nonrandom, it will generally be nonrandom for higher polynomials, even though the computer gives coefficients for the higher terms as requested by the programer. Coefficients of higher terms tend to alternate in sign and to be negligible in magnitude.

In addition to regression analysis we employ a technique developed by Šolc[21] whereby the computer determines one or two intersection temperatures for the two- or three-line fit that gives the lowest standard error. This is a completely objective method since the computer operator can have no influence on the results. A choice between two similar solutions is sometimes necessary. The minimum standard error from the two- or three-line fit is compared with the standard errors from linear and polynomial fits.

This program imposes a severe but justifiable penalty on the standard error, especially when the number of data points is small. It assumes in calculating standard error that two lines require five parameters (two slopes, two intercepts, and an intersection); three lines require seven parameters. By contrast, a quadratic has three parameters, a cubic, four. Even when a quadratic or cubic seems superior to a two- or three-line fit, on the basis of standard errors, residual patterns may, and generally do, rule out the polynomials.

If the data clearly follow two intersecting straight lines, the intersection can be calculated from the four parameters for the two lines. In the general case with considerable scatter in the data, an intersection within the range of data is assumed in making a comparison with a linear or quadratic model and hence the fifth parameter is considered essential.

Simha and his students[22] sometimes represent data above T_g as ln V_{sp}–T since the first derivative gives $\alpha = (1/V_{sp})(dV/dT)$ directly in units of K^{-1}. They appear to assume that α is constant above T_g, contrary to our findings with $\Delta\beta$. We have conducted regression analysis on ln V_{sp}–T data wherever possible and find that while R^2 is near unity and standard errors are small, the RES/SE patterns are distinctly nonrandom, in a manner characteristic of two straight lines. This is confirmed by the automatic intersection method. We prefer to work with β's and $\Delta\beta$'s and the related α's calculated therefrom. One example of a ln V_{sp}–T analysis is given for PnBMA in Table I.

I. V_{sp}–T Data at $P = 1$ bar

We have located eight sets of mercury dilatometer data and one set of density gradient tube data that can be used to estimate $\Delta\alpha$ at T_{II}. Values of $\Delta\alpha$ at T_g are always available from the original authors. These data sets are discussed in order of increasing T_g, which is generally the order of increasing T_{II}. Values of $\Delta\alpha$ at T_g given by the authors of the data and $\Delta\alpha$ at T_{II} from this paper are assembled later as Table IV.

Atactic Polypropylene (at-PP). Beck, Hiltz, and Knox[23] measured V_{sp}–T values on six specimens of at-PP whose crystallinities ranged from 0 to 10%. A double slope change at T_g and then at $T > T_g$ or T_{II} was found in all cases. Temperatures of the lower transition, namely, T_g, ranged from −13 to −20 °C; those for the upper break, which we identify with T_{II}, were from 24 to 35 °C. There were no tabulated V_{sp}–T values given. One specimen in particular, D-157, of zero crystallinity, was shown graphically in their Figure 3 while numerical expansivities were listed in their Figure 11, from which values of $\Delta\alpha$ at T_g and T_{II} given in Table IV were calculated. A prior critique of this set of data appears on p 536 of ref 6.

Poly(*n*-butyl methacrylate) (PnBMA). Because this polymer has a long liquid state with more than an average number of data points, it will be used to illustrate various computer techniques, whose results are collected in Tables I and II and in several figures, starting with Figures 1 and 2. Figure 3 illustrates the first step in our regression program,[18] namely, a linear model fitted to all data points. It is known from inspection of Figure 1 that this is not a correct model but the residuals pattern serves to define

Table I
Automatic Search for Intersections: PnBMA[a]

	intercept, $cm^3\ g^{-1}$	slope β,[b] $cm^3\ g^{-1}\ K^{-1}$	no. of data points	T_{ll}, °C	$T_{ll'}$, °C	std error,[b,c] $cm^3\ g^{-1}$	$\Delta\beta$,[b] $cm^3\ g^{-1}\ K^{-1}$
			A. Three-Line Fit (46.0-199.5 °C)				
line 1	0.9311	6.414	4				
line 2	0.9229	7.305	5	91.4	153.9	2.478	0.891
line 3	0.9147	7.837	4				0.532
			13				
			B. Two-Line Fit (46.0-146 °C)				
line 1	0.9311	6.414	4	91.36		2.048	0.891
line 2	0.9229	7.305	5				
			9				
			C. Two-Line Fit (46.0-160.2 °C)				
line 1	0.9307	6.482	5	97.34		2.179	0.917
line 2	0.9217	7.399	5				
		$\Delta\beta$ = 0.917	10				
			D. Quadratic (46.0-199.5 °C)				
			13			2.205	
			E. ln V_{sp}-T (46.0-160.2 °C)				
line 1	−0.07062	6.611	4	91.87		1.638	0.625[d-f]
line 2	−0.07636	7.236	6				
		$\Delta\alpha$ = 0.625	10				

[a] Computer method of Solc.[21] [b] Units of 10^{-4}. [c] The intersection temperature(s) T_{ll} and $T_{ll'}$ minimize the standard error in V_{sp} (calcd) assuming one, two, or three straight lines. The standard error is for the total number of data points. [d] This is $\Delta\alpha$ in units of $K^{-1} \times 10^{-4}$. [e] Standard error for a one-line fit is 6.234×10^{-4}. [f] Regression analysis shows that RES/SE values for a straight line are extremely nonrandom.

Table II
V_{sp}-T Regression Parameters for PnBMA at $T > T_g$[a]

model	temp range, °C	no. of data points	intercept, $cm^3\ g^{-1}$	slope β,[b] $cm^3\ g^{-1}\ K^{-1}$	std error in V_{sp}[b]	R^2 [c]
line 1	46.0-94.5	5	0.9307[d]	6.4818[d]	2.08	0.99978
line 2	105-160.2	5	0.9217[d]	7.3989[d]	3.32	0.99968
				$\Delta\beta$ = 0.9171		
quadratic 1	46.0-94.5	5			0.706	0.99998
quadratic 2	105-146.0	4			2.136	0.99991
quadratic 2	105-160.2	5			1.63	0.99995
quadratic	46-199.5	13			2.21	0.99997

[a] Methods described in ref 18. The residuals are slightly smaller and more random for the quadratic than for the linear fits. [b] Units of 10^{-4}. [c] Coefficient of correlation. [d] The calculated intercept (T_{ll}) for this pair of lines is 98.1 °C.

three regions of behavior separated by the transition temperatures T_{ll} and $T_{ll'}$. There are insufficient data points above $T_{ll'}$ to permit accurate regression analysis so that detailed analysis will concern the region from 46.0 to 160.2 °C.

Table I summarizes parameters from an automatic search for intersections for two and three straight lines. Also shown is the standard error for the quadratic fit from regression analysis. While the standard errors are close in all cases, they are marginally better for the two-line case, which defines T_{ll}. T_{ll} is between 91.4 and 97.3 °C. We have selected the actually measured point at 94.5 °C as being T_{ll}.

The final section in Table I is for ln V_{sp}-T data. While the standard error is the smallest one shown, regression analysis indicates an extremely nonrandom RES/SE pattern and hence we rejected this model.

Table II summarizes regression analysis parameters for two-line and two-quadratic fits in the T_{ll} region. The double-quadratic method is clearly better than the two-line method in regard to standard errors and marginally better with respect to R^2 and randomness of residuals. As a practical matter, each of the quadratics is scarcely distinguishable to the eye from straight lines. Hence we employ the values of the intersection temperature and $\Delta\beta$ for the two-line fits from Table I or II. For details of a similar case with poly(cyclopentyl methacrylate), see ref 18, p 1580 and Figure 12.

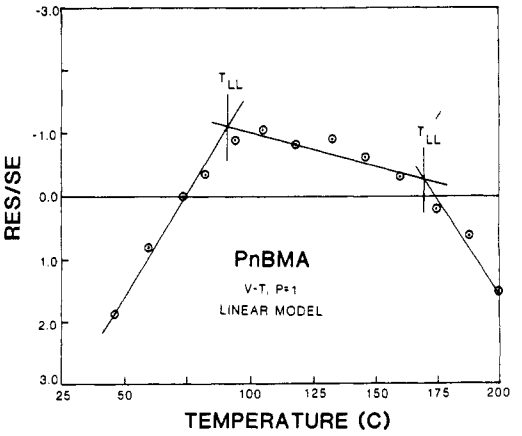

Figure 3. RES/SE pattern for a linear model applied to $T > T_g$ PnBMA data. The intersections locate transition temperatures T_{ll} and $T_{ll'}$.

While all sets of data were subjected to similar analyses, details will not be shown in general because the number

Table III
Comparative Studies of V_{sp}–T Data of Wilson-Simha[24] and Olabisi-Simha[5] for PcHMA[a]

	intercept, $cm^3\ g^{-1}$	slope,[b] $cm^3\ g^{-1}\ K^{-1}$	no. of data points	T_{ll}, °C	R^2 [c]	std error[b]	$\Delta\beta$,[b] $cm^3\ g^{-1}\ K^{-1}$
			A. Automatic Search[d]				
			Wilson-Simha				
line 1	0.8661	5.920	9	167.6		0.718	0.375
line 2	0.8598	6.295	11				
			Olabisi-Simha				
line 1	0.8694	5.699	4	163.7		1.365	0.512
line 2	0.8610	6.211	3				
			B. Regression Analysis				
			Wilson-Simha				
line 1	0.8661	5.920	9	168.4	0.99984	1.086[e,f]	0.373
line 2	0.8598	6.293	11		1.00000	1.086[e,f]	
quadratic			20			0.859[e]	
			Olabisi-Simha				
line 1	0.8694	5.699	4		0.99946	2.494	
line 2			33[g]			0.864	
quadratic			7			0.864	

[a] Polymer specimen same; Wilson-Simha presented smoothed data at 5 K intervals at P = 1 bar; Olabisi-Simha presented raw data at irregular intervals at P = 1 bar and $P > 1$ bar. [b] Units of 10^{-4}. Standard error is smaller the larger the number of data points and usually favors a quadratic over two lines. [c] Coefficient of correlation. [d] Automatic search method provides slopes, incercepts intersection temperature for two lines, and standard error for both sets of data. It does not calculate R^2 and does not provide residuals. [e] Residuals are nonrandom. [f] Two quadratics for lines 1 and 2 make the residuals more random. [g] Program will not calculate a regression line for three data points.

of data points was fewer in most cases than for PnBMA.

Poly(vinyl acetate) (PVAc). McKinney and Goldstein[11] tabulate liquid-state values of V_{sp} at 5 K intervals from 35 to 100 °C at P = 0. The raw data were subjected by the authors to a computer smoothing technique and hence the table contains only the smoothed values at exactly the 5 K intervals. It is not known to what extent this smoothing has altered the sharpness of T_{ll}. We have estimated T_{ll} at 70 °C at P = 1 bar, with a change in expansivity $\Delta\beta = 0.101 \times 10^{-4}$ or $\Delta\alpha = 0.221 \times 10^{-4}$, which appears later in Table IV along with a value of $\Delta\alpha$ at T_g of $4.141 \times 10^{-4}\ deg^{-1}$ given in ref 11.

Isotactic Poly(methyl methacrylate) (it-PMMA). The V_{sp}–T data of Wilson and Simha[24] as well as that of Quach, Wilson, and Simha[25] fail to reveal a slope change near T_{ll} even though the latter shows strong evidence for T_{ll} in part II ($P > 1$ bar) and in V–P isothermal data reported in ref 2.

Density gradient tube data of Bywater and Toporowski[26] on a 60% isotactic–40% syndiotactic PMMA sample has been studied by regression analysis with the three-line parameters listed in Table II of ref 6 and the V_{sp}–T plot shown as Figure 8 of ref 6.

Poly(cyclopentyl methacrylate) (PcPMA). Smoothed dilatometric V_{sp}–T data have been published by Wilson and Simha,[24] who reported a transition above T_g, which they considered to be a liquid–liquid transition. We have confirmed this conclusion by an exhaustive regression analysis study,[18] which provides the value of $\Delta\alpha$ listed in Table IV.

Atactic Polystyrene (at-PS). Hellwege et al.[27] did not report V_{sp} data at P = 1 bar on a specimen of thermal PS having an apparent high volatile content (T_g = 89 °C). The V_{sp}–T data of Quach and Simha[22] do not reveal a slope change in the T_{ll} region, in part because the liquid range is short and in part because $\Delta\alpha$ is quite small for PS.

Höcker, Blake, and Flory[28] studied an anionic PS of M_n = 51 000 in a high-precision mercury dilatometer, using specimen weights of 45–50 g, in contrast to the 3–5 g normally employed. They reported an apparent third-order transition in $(1/V)/(dV/dT)$ vs. T plots near 170 °C, using the point-to-point derivative method. Since this transition temperature is in the T_{ll} range for anionic PS, we must assume that they confirm the existence of T_{ll} by thermal expansion. These data have been discussed by us in a different context elsewhere, where detailed background on the specimens and regression analysis are provided. (See p 531 and Figure 28 of ref 6 or p 737 and Figure 6 of ref 8.)

These data are another example of an apparent two-straight-line fit to V_{sp}–T across T_{ll} which in fact gives nonrandom residuals. A pair of mild quadratics intersecting near 160 °C is a more accurate model, as first noticed in connection with Figure 6 of ref 8.

Richardson and Savill[29] have reported precision mercury dilatometric data on a series of anionic PS's. They represented their data above T_g by a quadratic and state explicitly that they find no evidence for a T_{ll}. Their specimen weights were usually less than 5 g, in contrast to the much larger specimen of Höcker et al.[28] Since tabulated V_{sp}–T data were not provided in ref 31, we could not test their conclusions by regression analysis.

Atactic Poly(methyl methacrylate) (at-PMMA). Neither the data of Hellwege et al.[27] nor that of Olabisi and Simha[5] go above the T_{ll} region of this polymer. Evidence for the existence of T_{ll} by a variety of other methods has been summarized in Table III of ref 6.

Poly(cyclohexyl methacrylate) (PcHMA). Two sets of V_{sp}–T data are available: (a) the smoothed values of Wilson and Simha,[24] with 20 data points at 5 K intervals above T_g from 120 to 220 °C and (b) the unsmoothed data of Olabisi and Simha[5] at seven temperatures above T_g. These P = 1 bar data are part of a total set of P–V–T data whose isothermal V_{sp}–P results show evidence for T_{ll} (Figures 15 and 16 of ref 6). These two sets of data provide an opportunity to compare results by two sets of authors with different methods of data handling. Table III collects the various parameters by automatic intersection search in part A and regression analysis in part B. Both programs suggest for the Wilson–Simha data the possibility of a second event near 188 °C, which may indicate the beginning of thermal decomposition or might indicate $T_{ll'}$.

Table IV
Summary of Thermal Expansion Results at P = 1 bar

polymer[a]	T_g, °C	$\Delta\alpha$ at T_g,[b] deg^{-1} × 10^4	ref[c]	T_{ll},[d] °C	T_{ll} (K) / T_g (K)	$\Delta\alpha$ at T_{ll}[e]	$\Delta\alpha$ at T_g[f] / $\Delta\alpha$ at T_{ll}	other P-V-T sources
at-PP	−15	5.2	23	25	1.16	1.1	4.7	none
PnBMA	20	1.69[g]	5	95	1.26	0.89	1.9	*m, o, p*
PVAc	30	4.14	11	85	1.18	0.221	21.7	*m, p*
it-PMMA	47	3.49	25	110[h]	1.20	*h*	*h*	*m, o, p*
60% it-PMMA	58	3.71	*i*	121[i]	1.19	1.29	3.4	none
PcPMA	75	2.88	24	148	1.21	0.716	4.0	none
at-PS	100	3.03	28[j]					
sample 1, 1st heat				162.6	1.17	0.212	14.3	none
sample 2, 2nd heat				164.4	1.17	0.231	13.1	none
at-PMMA	105	3.44	5	160–165[k]	1.15	*k*	*k*	none
PcHMA	107	3.38	5	165	1.15	0.491	6.9	*m, o, p*
		2.98	24	167.4	1.16	0.386	7.72	none
PoMS	131	2.71	22	171	1.10	0.11[l]	24.6	*n, p*
				175	1.11			*o*

[a] Arranged in order of increasing T_g. A $T > T_g$ transition was noted by the original authors only in the case of ref 23, 24, and 28. [b] $\Delta\alpha$ at T_g is $\alpha_l - \alpha_g$. [c] Source of T_g and $\Delta\alpha$ at T_g. [d] Either from this report or sources cited in the text. [e] $\Delta\alpha$ at T_{ll} in units of 10^{-4} deg^{-1} from this report. [f] This ratio is used as a measure of the relative strengths of T_g and T_{ll}. [g] This abnormally small value of $\Delta\alpha$ is a consequence of a large $T > T_g$ transition from the *n*-butyl side group as first noted by Simha and Boyer.[15] [h] T_{ll} is obtained from a variety of sources, i.e., ref 2, 3, and 32. $\Delta\alpha$ at T_{ll} is zero or vanishingly small. [i] Table I of ref 6. [j] T_g is conventional value and $\Delta\alpha$ at T_g comes from $\Delta\alpha T_g$ = 0.113. Authors of V-T data in ref 28 worked only above T_g. [k] T_{ll} observed by a variety of methods listed in Table III of ref 3. No thermal expansion data were located above T_{ll}. [l] There were only three isotherms above T_{ll}. [m] Isothermal V-P data in ref 1, 2, or 6. [n] From isothermal V-P inpublished data. [o] From b vs. T at $P \leq 400$ bars in ref 3. [p] See also section on $P > 1$ bar. ln V_{sp}-T plots have been analyzed where data permitted, namely, on the PnBMA, 60% it-PMMA, PcPMA, at-PS, and PoMS polymers. All are characterized by $R^2 \rightarrow 1.0$, standard errors very low, but nonrandom residuals patterns.

Poly(*o*-methylstyrene) (PoMS). Quach–Simha[22] data for seven isotherms above T_g at P = 1 bar were employed. The b vs. T study[3] suggested $T_{ll} \sim 175$ °C, with some uncertainty because there were only three higher isotherms from 179 to 197 °C. The automatic intersection search with V_{sp}–T data placed T_{ll} at 171 °C at P = 1 bar and at 176 °C at P = 100 bars; there was no detectable slope change at P = 200 bars. An approximate value of $\Delta\alpha$ at P = 1 bar is listed in Table IV. Quach and Simha reported T_g(LP) values at several pressures.

Summary of Results at P = 1 bar. Table IV assembles values of $\Delta\alpha$ at T_g, $\Delta\alpha$ at T_{ll}, their ratios, and several other pertinent quantities. It is clear at once that the T_{ll} transitions for PS, PoMS, and PVAc are extremely weak compared to T_g. The several methacrylates are relatively strong, with at-PP occupying an intermediate position. We suggest that the methacrylates are comparatively strong because of chain stiffness and polarity. This is consistent with the hypothesis about the origin of T_{ll} proposed by Frenkel and Baranov (see pp 540ff of ref 6). It is ironic that so much effort has been extended in studying T_{ll} of PS, primarily because of the ready availability of narrow molecular weight distribution specimens, which are well characterized. We are currently concentrating attention on polymers of alkyl and cycloalkyl methacrylates, especially by differential scanning calorimetry.

II. T_{ll} from Isobaric V-T Data at $P > 1$ bar

The behavior of $\Delta\beta$ at $P > 1$ bar represents a competition between the normal tendency for β to increase with temperature above T_{ll} as seen in part I and the suppressing effect of pressure because of an increase in the temperature coefficient of compressibility above T_{ll} discussed in ref 3. $\Delta\beta$ at T_{ll} exhibits either of three behavior habits with increasing P: (1) $\Delta\beta$ changes from plus to zero to minus, as found in the case of PnBMA; (2) $\Delta\beta$ changes from plus to zero (PcHMA); or (3) $\Delta\beta$ starts at or near zero and becomes negative (it-PMMA, PS). These patterns are influenced by (a) the top isotherms and top pressures employed, (b) the fact that T_{ll} increases with pressure, and

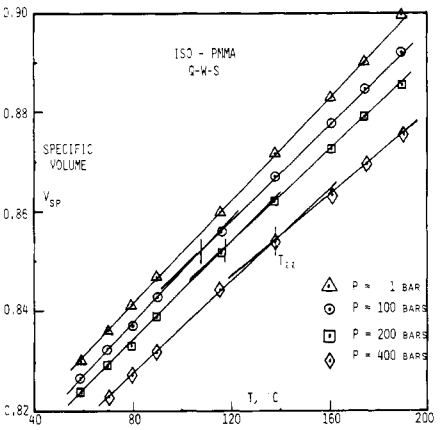

Figure 4. Specific volume–temperature plots for it-PMMA at the indicated pressures in bars showing T_{ll} moving out of range. Data of Quach, Wilson, and Simha.[25]

(c) the presence of other transitions such as T_g(LP) possessing associated $\Delta\beta$'s that may be stronger than that of T_{ll}. Some typical examples will now be discussed.

A plot of β_{ll} against P showing that $\Delta\beta$ is already zero at P of about 500 bars appears as Figure 1 of ref 1. Figure 13 of ref 6 applies quadratic regression lines to these same data, showing three patterns: (a) concave upward between 1 and about 400 bars; (b) linearity up to about 1000 bars; and concave downward at higher pressures. These quadratic patterns are approximations to the actual data and were used for illustrative purposes only.

Techniques of data handling are as in part I, complicated by the two facts that as T_{ll} increases with P, the number of available temperatures above T_{ll} decreases while the slope change, $\Delta\beta$, decreases. Also, several sets of tabulated data become available in the form of $1 - V/V_0$ vs. T, where V_0 is the specific volume at P = 0 and V the specific volume at pressure P.

Figure 4 is a plot of V_{sp}–T at several pressures for the it-PMMA data of Quach, Wilson, and Simha.[25] Intersection pressures were determined by the automatic search

Table V
Summary of Thermal Expansion Parameters at $P > 1$ bar

polymer	pressure, bars	T_g,[a] °C	$\Delta\alpha$ at T_g,[b] 10^{-4} K^{-1}	T_{II},[c] °C	$\Delta\alpha$ at T_{II},[d] 10^{-4} K^{-1}	$\frac{\Delta\alpha \text{ at } T_g}{\Delta\alpha \text{ at } T_{II}}$	T_{II}/T_g
PnBMA	1	20	2.08	95[g,h]	0.99	2.1	1.26
	100	22	2.23	100[g,i]	0.96	2.3	1.26
	200	24	2.39	104[g]	0.70	3.41	1.27
	300	26	2.2	112[g]			1.29
at-PS	80	87[e]	3.1[f]	148[j]	0.302	10.3	1.17
PcHMA	1	107	3.50	156[k]	0.49	7.1	1.13
	100	109	3.42	160[k]	0.35	9.8	1.13
	200	111	3.20	165[k]	0.29	11	1.14
	300	114	2.99	170[k]	0.27	11	1.14
PVAc	0-1000[l]						
PS	0-2000[l]						
it-PMMA	1-2000[l]						
PoMS	1-2000[l]						

[a] Estimated from T_g at $P = 1$ bar and dT_g/dP using values in ref 5, except for PS. [b] Estimated from ln V_{sp}-T plots at each pressure, with details as in the text, except for PS. [c] Methods as shown for each value. [d] Calculated from $\Delta\beta$ values obtained via regression analysis of V_{sp}-T data at indicated pressures. [e] From Figure 7 of ref 27 at $P = 0$ (pressures in (kg P)/cm^2. [f] calculated from $0.113/T_g$. [g] Estimated visually from intersections of Figure 5. [h] Calculated intersection of regression lines is 94.1 °C. [i] Calculated intersection of regression lines is 97.4 °C. [j] Calculated from intersection of regression lines. [k] Estimated visually from intersections of V_{sp}-T plots not shown. [l] Intersection temperatures estimated for some isobars from V_{sp}-T or $(1 - V/V_0)$-T plots (see text).

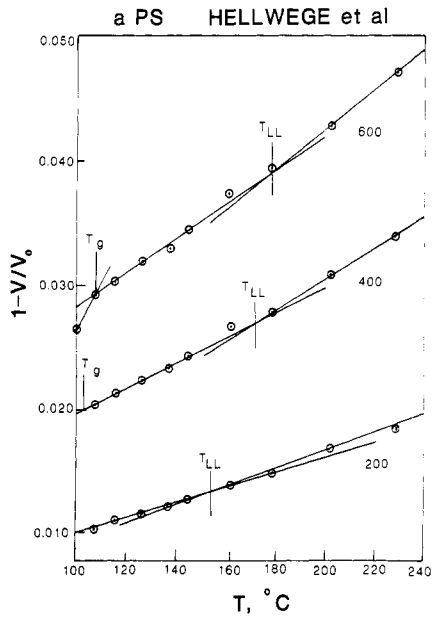

Figure 5. Plots of $1 - V/V_0$ for at-PS at the indicated pressures in kg cm^{-2} from the data of Hellwege, Knappe, and Lehmann[27] showing T_{II}.

method of Šolc described earlier. At higher pressures, there is no evidence for T_{II} but negative slope changes at T_g(LP) are evident. Figure 5 shows a plot of $1 - V/V_0$ at 200, 400, and 600 bars based on the data of Hellwege et al.[27] for an atactic polystyrene. The location of T_g is indicated. They also reported V_{sp}-T data at the single pressure of 80 bars. This plot is not shown but the T_{II} obtained is given in Table V.

Beret and Prausnitz[31] report for PVAc V/V_0 values for six isotherms from 64 to 120 °C and pressures from 0 to 1000 bars. Plots of $1 - V/V_0$ against T indicate weak slope changes at 200 and 300 bars but not at 100 bars or at higher pressures. The PVAc data of McKinney and Goldstein[11] provided no evidence for T_{II} at $P > 1$ bar, probably because of the inherent weakness of T_{II} in PVAc, but possibly complicated by their data-smoothing procedure.

Plots of $1 - V/V_0$ vs. T (not shown) for PIB, using the data of Beret and Prausnitz, showed evidence for a possible transition in the range 600–1000 bars. With only five temperatures available from 52 to 110 °C, such intersections were not well defined. However, they agreed rather closely with calculated values of T_{II} using results from ref 1, namely, $T_{II} = 264$ K at $P = 1$ bar and $dT_{II}/dP = 120$ K/kbar.

V_{sp}-T plots for PnBMA above T_g for $P = 100$–400 bars were prepared but are not shown. A weak $T_{II'}$ is evident at about 185 °C at $P = 100$ bars but is either out of range or suppressed at 200 bars. T_{II} is still evident at 300 bars but is no longer apparent at 400 bars.

We also prepared V_{sp}-T plots for PcHMA from 1 to 800 bars, showing T_{II} scarcely evident at 300 bars, zero at 400 and 600 bars, and essentially out of range at 800 bars. V_{sp} values at 169.3 °C are consistently high for all isobars and have been ignored both in drawing straight lines and in computer calculations.

Table V collects values of $\Delta\alpha$ at T_g and $\Delta\alpha$ at T_{II} (both determined by us) for PnBMA, at-PS, and PcHMA. The procedure presented earlier of calculating β_I and β_{II} from regression analysis was employed. The apparent increase in $\Delta\alpha$ at T_g for PnBMA is a consequence of (a) a small number of data points below T_g and (b) the inherent weakness of T_g in this polymer, as noted earlier. Since $\Delta\alpha$ at T_{II} is more sensitive to pressure than is $\Delta\alpha$ at T_g, the ratios in the next-to-last column increase with P in the expected manner. The ratio for PS at $P = 80$ bars is higher than the value in Table IV at $P = 1$ bar. This may result from the high volatile content of this material used by Hellwege et al.

Discussion of Overall Results

Figure 6 summarizes T_{II}-P results for the polymers under study. Several sources were employed as indicated in the caption to the figure: T_{II} at $P = 1$ bar from Table IV, except where noted; low-pressure T_{II} values from Table V or Figures 4 and 5; and high-pressure T_{II} values calculated from the linear form of the Tait equation

$$Y = \exp[(1/C')(1 - V/V_0)] - 1 = P/b \qquad (2)$$

where $C' = 0.0894$. Details of this method will be given elsewhere[32] but briefly, a linear least-squares line constrained to pass through the origin, $P = 1$, $P/b = 0$, is computer drawn, and values of RES/SE are calculated as in Figure 2 or 3 for V_{sp}-T data. In general, the RES/SE values are nonrandom about zero, indicative of two or more lines needed to represent the $Y = P/b$ vs. P data. Inter-

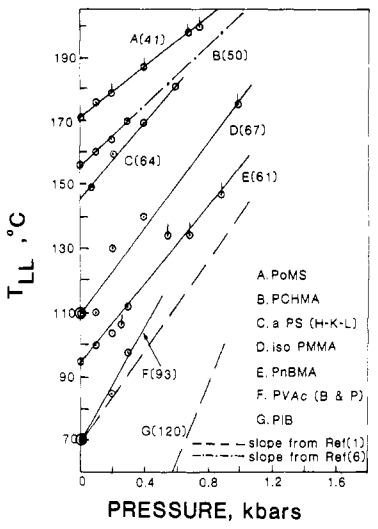

Figure 6. Combined used of isobaric V–T data at low pressures and isothermal V–P data at intermediate pressures for the indicated polymers. Numbers in parentheses are slopes in K/kbar. Plain circles, V–T; pips up, V–P based on eq 4; double circles, at $P = 0$ from b vs. T plots in ref 3; dashed lines are slopes from ref 1 and 6.

section pressures are located in the P/b vs. P plots, using the automatic two- or three-line search method of Šolc.[21] This method was employed for PoMS; it did not work for PcHMA because of interference from the T_g(LP) transition; it worked for PnBMA as shown in Figure 6 but only if pressures from 1 to 1000 bars were employed so as to avoid interference from T_g(LP). T_{ll} at higher pressures for PcHMA are indicated by drawing the slope from Figure 16 of ref 6, where T_{ll} values were determined from isothermal ln V_{sp}–P plots as recommended in ref 1. The values of T_{ll} at $P \rightarrow 0$ for it-PMMA and PVAc are from b–T plots in ref 3. The dashed line for PVAc shows the slope determined in ref 1 from isothermal V–P data. The higher slope from $1 - V/V_0$ vs. T plots may be more accurate because it was noted that dT_{ll}/dP values vary inversely as T_g. The dashed line G for PIB from ref 1 has the highest dT_{ll}/dP value yet observed.

Figure 6 illustrated the complementary nature of isothermal V–P and isobaric V–T studies in delineating the pressure dependence of T_{ll}. Both methods would gain accuracy if the isotherms and the isobars were more closely spaced.

Summary and Conclusions

1. Values of the change in coefficient of expansion, $\Delta\alpha$, across the liquid–liquid transition temperature, T_{ll}, were calculated by regression analysis techniques for eight amorphous polymers at $P = 1$ bar (see Table IV).

2. These $\Delta\alpha$'s at T_{ll} are compared with $\Delta\alpha$'s at T_g. $\Delta\alpha$ at T_g is some 2–25 times stronger than at T_{ll}. The ratio is highest for PS, PoMS, and PVAc, lowest for the poly(alkyl and cycloalkyl methacrylates), and intermediate for atactic polypropylene.

3. Values of $\Delta\alpha$ across T_{ll} at 1 bar $< P \leq 400$ bars were estimated for PS, PcHMA, and PnBMA and were expectedly smaller than for $P = 1$ bar.

4. T_{ll} could be obtained graphically as a function of pressure at $P \leq 600$ bars for PS, it-PMMA, PcHMA, PVAc, and PIB, using isobaric plots of V_{sp}–T or $(1 - V/V_0)$–T at several low pressures.

5. Plots of T_{ll} as a function of P are shown for six different polymers (see Figure 6). The locus of T_{ll}–P from ref 1 is indicated.

6. The slopes, dT_{ll}/dP, agree reasonably well with values obtained by isothermal V–P methods used earlier in refs 1 and 2.

7. In addition to T_{ll}, the locus of the low-pressure glass transition, T_g(LP), could be detected in some isobars for it-PMMA, PoMS, and PcHMA. A $T > T_{ll}$ transition designated $T_{ll'}$ was found in the case of PnBMA and PcHMA.

8. T_{ll} from isobaric V–T data at low pressure provides thermodynamic-type evidence for the liquid–liquid transition, just as in the case of T_g.

9. The T_{ll} values at $P \leq 600$ bars obtained herein complement a range of the T_{ll}–P regime not always well defined from isothermal V–P data.

10. These studies show that V_{sp}–T data for the liquid state above T_g do not follow quadratic or cubic polynomials exactly. Rather, the data from low to high temperature appear to follow any of several paths: two straight lines, two quadratics, or one straight line and a quadratic or vice versa. However, quadratics or cubics generally are convenient representations of the data for engineering calculations.

Acknowledgment. This study was suggested by Professor G. Rehage, Institute of Physical Chemistry, Clausthal-Zellerfeld. We are indebted to S. E. Keinath and K. M. Panichella for regression analysis studies and to K. M. Panichella for the artwork. Development of a special computer technique by Dr. K. Šolc of MMI has been of considerable assistance in data analysis.

References and Notes

(1) Boyer, R. F. *Macromolecules* **1981**, *14*, 376.
(2) Boyer, R. F. *Colloid Polym. Sci.* **1980**, *258*, 760.
(3) Boyer, R. F. *Macromolecules* **1982**, *15*, 774.
(4) This procedure was proposed by K. Šolc, MMI, with regression analysis studies carried out by S. E. Keinath and K. M. Panichella of MMI. A manuscript is in preparation.
(5) Olabisi, O.; Simha, R. *Macromolecules* **1975**, *8*, 206.
(6) Boyer, R. F. *J. Macromol. Sci., Phys.* **1980**, *B18*, 461.
(7) Gillham, J. K.; Boyer, R. F. *J. Macromol. Sci., Phys.* **1977**, *B13*, 497.
(8) Boyer, R. F. *Polym. Eng. Sci.* **1979**, *19*, 732.
(9) Boyer, R. F. *Eur. Polym. J.* **1981**, *17*, 661.
(10) Gee, G. *Polymer* **1966**, *7*, 177.
(11) McKinney, J. E.; Goldstein, M. *J. Res. Natl. Bur. Stand., Sect. A* **1974**, *75A*, 331.
(12) Haldon, R. A.; Schell, W. J.; Simha, R. *J. Macromol. Sci., Phys.* **1967**, *B1*, 759.
(13) Haldon, R. A.; Simha, R. *J. Appl. Phys.* **1968**, *39*, 1890.
(14) Haldon, R. A.; Simha, R. *Macromolecules* **1968**, *1*, 340.
(15) Simha, R.; Boyer, R. F. *J. Chem. Phys.* **1962**, *37*, 1003.
(16) Simha, R.; Weill, G. E. *J. Macromol. Sci., Phys.* **1970**, *B4*, 215.
(17) Boyer, R. F.; Simha, R. *J. Polym. Sci., Polym. Lett. Ed.* **1973**, *11*, 33.
(18) Boyer, R. F.; Miller, R. L.; Park, C. N. *J. Appl. Polym. Sci.* **1982**, *27*, 1565.
(19) Anscombe, F. J.; Tukey, J. W. *Technometrics* **1963**, *5*, 141.
(20) Tukey, J. W. "Exploratory Data Analysis"; Addison-Wesley: Reading, MA, 1977.
(21) Šolc, K., MMI, unpublished results.
(22) Quach, A.; Simha, R. *J. Appl. Phys.* **1971**, *42*, 4592.
(23) Beck, D. A.; Hiltz, A. A.; Knox, J. R. *SPE Trans.* **1963**, *3*, 279.
(24) Wilson, P. S.; Simha, R. *Macromolecules* **1973**, *6*, 902.
(25) Quach, A.; Wilson, P. S.; Simha, R. *J. Macromol. Sci., Phys.* **1974**, *B9*, 533.
(26) Bywater, S.; Toporowski, P. M. *Polymer* **1972**, *13*, 94.
(27) Hellwege, K. H.; Knappe, W.; Lehmann, P. *Kolloid Z. Z. Polym.* **1962**, *183*, 110.
(28) Höcker, H.; Blake, G. J.; Flory, P. J. *Trans. Faraday Soc.* **1971**, *67*, 2251.
(29) Richardson, M. J.; Savill, N. G. *Polymer* **1977**, *18*, 3.
(30) Boyer, R. F.; Denny, Lisa R.; Elias, H.-G.; Gillham, J. K. *Org. Coat. Plast. Chem.* **1980**, *42*, 682.
(31) Beret, S.; Prausnitz, J. J. *Macromolecules* **1975**, *8*, 536.
(32) Šolc, K.; Keinath, S. E. Boyer, R. F., manuscript in preparation for *Macromolecules*.